RAA 2019 Vol. **19** No. **5**, 63(14pp) doi: 10.1088/1674–4527/19/5/63

http://www.raa-journal.org *http://iopscience.iop.org/raa*

Research in Astronomy and Astrophysics

INVITED REVIEWS

The Energy Sources of Superluminous Supernovae

Shan-Qin Wang[1,2,3], Ling-Jun Wang[4] and Zi-Gao Dai[1,3]

[1] School of Astronomy and Space Science, Nanjing University, Nanjing 210093, China; *dzg@nju.edu.cn*
[2] Guangxi Key Laboratory for Relativistic Astrophysics, School of Physical Science and Technology, Guangxi University, Nanning 530004, China; *shanqinwang@gxu.edu.cn*
[3] Key Laboratory of Modern Astronomy and Astrophysics (Nanjing University), Ministry of Education, Nanjing 210093, China
[4] Astroparticle Physics, Institute of High Energy Physics, Chinese Academy of Sciences, Beijing 100049, China

Received 2018 December 11; accepted 2019 January 25

Abstract Supernovae (SNe) are the most brilliant optical stellar-class explosions. Over the past two decades, several optical transient survey projects discovered more than $\sim$ 100 so-called superluminous supernovae (SLSNe) whose peak luminosities and radiated energy are $\gtrsim 7 \times 10^{43}\,\mathrm{erg\,s^{-1}}$ and $\gtrsim 10^{51}$ erg respectively, at least an order of magnitude larger than those of normal SNe. According to their optical spectra features, SLSNe have been split into two broad categories of type I that are hydrogen-deficient and type II that are hydrogen-rich. Investigating and determining the energy sources of SLSNe would be of outstanding importance for understanding their stellar evolution and explosion mechanisms. The energy sources of SLSNe can be determined by analyzing their light curves (LCs) and spectra. The most prevailing models accounting for the SLSN LCs are the ^{56}Ni cascade decay model, the magnetar spin-down model, the ejecta-circumstellar medium interaction model and the jet-ejecta interaction model. In this *review*, we present several energy-source models and their different combinations.

Key words: stars: magnetars — supernovae: general

1 INTRODUCTION

Supernovae (SNe) are believed to be violent explosions of massive stars or white dwarfs. The peak luminosities and radiated energies of normal SNe are $\sim 10^{42} - 10^{43}\,\mathrm{erg\,s^{-1}}$ and $\sim 10^{49}$ erg, respectively. According to their optical spectra around the peaks, SNe can be divided into type I whose spectra lack hydrogen lines and type II whose spectra show hydrogen lines (Minkowski 1941; Filippenko 1997).

Over the past two decades, several sky-survey projects for optical transients have discovered about 100 ultra-luminous SNe (e.g., Quimby et al. 2011; Chomiuk et al. 2011; Nicholl et al. 2014; Quimby 2014; De Cia et al. 2018; Lunnan et al. 2018) whose peak luminosities and radiated energies are $\gtrsim 7 \times 10^{43}\,\mathrm{erg\,s^{-1}}$ (absolute magnitudes in any band must be $\lesssim -21$ mag (Gal-Yam 2012) [1]) and $\gtrsim 10^{51}$ erg, respectively. These highly luminous SNe are coined "superluminous supernovae (SLSNe)" (for reviews focusing on observations, see Gal-Yam 2012, 2018).

Like normal SNe, SLSNe can be divided into types I (hydrogen-poor) and II (hydrogen-rich). To date, almost all type I SLSNe have been helium-deficient and are therefore type Ic. The spectra of most type I SLSNe resemble those of SNe Ic (Pastorello et al. 2010; Gal-Yam 2012; Inserra et al. 2013; Nicholl et al. 2016b), especially those of SNe Ic-BL (Liu et al. 2017b). Most SLSNe II are SLSNe IIn whose spectra have narrow- and intermediate-width Hα emission lines (Smith et al. 2007), similar to those of SNe IIn (Schlegel 1990, 1996; Filippenko 1997). The prototype SLSN IIn is SN 2006gy (Smith et al. 2007). So far, only two confirmed SLSNe are of type IIL: SN 2008es (Gezari et al. 2009; Miller et al. 2009) and SN 2013hx (Inserra et al. 2018). The similarity between SLSNe Ic/IIn and SNe Ic-BL/IIn indicates that SLSNe likely originate from the

[1] Gal-Yam (2018) suggests that the threshold can be set to be $M_g < -19.8$ mag.

explosions of massive stars since SNe Ic-BL/IIn are also believed to be produced by the explosions of massive stars.

According to the characteristics of their light curves (LCs), most SLSNe I can be divided into two groups: fast-evolving (Quimby et al. 2011; Inserra et al. 2013; Nicholl et al. 2014) and slowly-evolving ones (Gal-Yam et al. 2009; Nicholl et al. 2013, 2016a; Inserra et al. 2017). However, the LC behaviors of SLSNe are rather heterogeneous and some SLSNe can be classified into neither fast-evolving nor slowly-evolving cases (e.g., Gaia16apd Nicholl et al. 2017b; Kangas et al. 2017; Yan et al. 2017), being transitional objects between these two types. The LCs of some SLSNe I show double-peaked structure (Nicholl et al. 2015; Nicholl & Smartt 2016; Smith et al. 2016; Vreeswijk et al. 2017). While the LCs of SLSNe II are more complicated than those of SLSNe I, all of them do not show double-peaked structure.

SLSNe tend to explode in low-metallicity dwarf galaxies (Young et al. 2010; Neill et al. 2011; Chen et al. 2013; Lunnan et al. 2014, 2015) and the star formation rates (SFRs) of the host galaxies of SLSNe are usually high. To date, only very few SLSNe have been found in giant, metal-rich galaxies, e.g., SN 2006gy (Smith et al. 2007) and SN 2017egm (Nicholl et al. 2017a; Bose et al. 2018).

Determining the energy sources powering the LCs of SLSNe is of outstanding importance for understanding the stellar evolution and explosion mechanisms. We can conclude that the LCs of most ordinary SNe must be powered by ^{56}Ni cascade decay (e.g., Colgate & McKee 1969; Colgate et al. 1980; Arnett 1982; Cappellaro et al. 1997; Valenti et al. 2008; Chatzopoulos et al. 2012; Piro & Nakar 2013), and/or ionized hydrogen recombination (e.g., Popov 1993; Dessart & Hillier 2005; Kasen & Woosley 2009), and a minor number of SNe might be powered by ejecta–circumstellar medium (CSM) interaction (e.g., Chevalier 1982; Chevalier & Fransson 1994; Chugai & Danziger 1994; Chugai 2009) or neutron-star/magnetar spin-down (Ostriker & Gunn 1971; Maeda et al. 2007). Unlike ordinary SNe, the energy sources of SLSNe are still elusive and under debate. To date, the most promising energy-source models accounting for the SLSN observations are the pair instability SN model (Barkat et al. 1967; Rakavy & Shaviv 1967; Heger & Woosley 2002; Heger et al. 2003) which is essentially the ^{56}Ni cascade decay model but the required ^{56}Ni ($\gtrsim 5\,M_{\odot}$) is significantly larger than that for powering ordinary SNe ($\lesssim 0.6\,M_{\odot}$), the magnetar model (Kasen & Bildsten 2010; Woosley 2010; Chatzopoulos et al. 2012, 2013b; Inserra et al. 2013; Chen et al. 2015; Wang et al. 2015b, 2016b; Dai et al. 2016), the ejecta–CSM interaction model (Chevalier & Irwin 2011; Chatzopoulos et al. 2012; Liu et al. 2018) and the fallback (jet-ejecta interaction) model (Dexter & Kasen 2013). All these models suppose that the released high-energy photons get absorbed and heat the ejecta, eventually becoming ultraviolet (UV)–optical–near infrared (NIR) emission. In this *review*, we describe these energy-source models and their combinations, and discuss their implications for SLSNe.

2 SINGLE ENERGY-SOURCE MODELS

The energy-source models interpreting the unique peak (for single-peaked LCs) or the second peak (for double-peaked LCs) of SNe (and SLSNe) are mainly the ^{56}Ni model, the magnetar model, the ejecta-CSM interaction model and the fallback (jet-ejecta interaction) model. In some cases, the combinations of two or three energy sources must be taken into account. In this section, we focus on the single energy-source model based on the semi-analytic descriptions.

2.1 The ^{56}Ni Model

When massive stars explode as Fe-core core-collapse SNe (CCSNe, Baade & Zwicky 1934; Janka et al. 2007; Janka 2012), they launch energetic shocks which can heat the stellar mantles to a temperature $\gtrsim 5\times10^{9}$ K. Shock-heated silicon shells would synthesize a great amount of radioactive elements, e.g., ^{56}Ni, ^{57}Ni, ^{44}Ti, ^{22}Na, etc. At early epochs ($\lesssim 500$ days), the power coming from ^{56}Ni is significantly larger than that released by all other elements (Lundqvist et al. 2001; Sollerman et al. 2002). Due to the large distance, many SLSNe and luminous SNe lack late-time photometric observations. The contribution from ^{57}Ni, ^{44}Ti and ^{22}Na can therefore be neglected in modeling the LCs of these SNe and the radioactive-powered model produces the same results as the ^{56}Ni-powered model.

We plot some LCs powered by different amounts of ^{56}Ni in Figure 1. By fixing κ (the optical opacity of the ejecta) $=\ 0.1\,\mathrm{cm^2\,g^{-1}}$, $v_{\rm sc}$ (the scale velocity of the ejecta) $=\ 10^9\,\mathrm{cm\,s^{-1}}$, κ_γ (the gamma opacity of the ejecta) $=0.027\,\mathrm{cm^2\,g^{-1}}$, and setting $M_{\rm ej}$ (the mass of the ejecta) $=\ 5, 10, 50\,M_{\odot}$ and $M_{\rm Ni}$ (the mass of ^{56}Ni) $=$ $0.1, 0.5, 5.0\,M_{\odot}$, we plot 12 LCs, three of which are ^{56}Ni cascade decay input LCs and nine of which are SN LCs powered by ^{56}Ni cascade decay. Adopting this set of parameters, Figure 1 shows that the ^{56}Ni model can reasonably explain normal SNe, but it is difficult to use it to explain the LCs of SLSNe ($L_{\rm peak}\ \gtrsim\ 7\times10^{43}\,\mathrm{erg\,s^{-1}}$) since the ratios of $M_{\rm Ni}$ to $M_{\rm ej}$ are unreasonably large

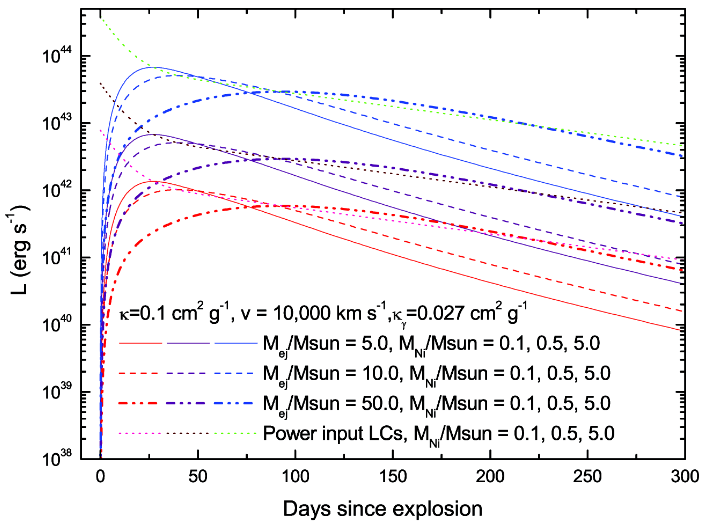

Fig. 1 LCs powered by ^{56}Ni cascade decay. We fix κ =0.1 cm^2 g^{-1} and $v_{\rm sc}$ = 10^9 cm s^{-1}. The LCs powered by the same amount of ^{56}Ni are represented by the same colors.

($5.0/5.0 = 1$, $5.0/10.0 = 0.5$ for the two most luminous LCs).

Being more luminous than ordinary SNe by a factor of $\sim 10 - 100$ or more, the required ^{56}Ni is usually (significantly) larger than $\sim 5\,M_\odot$ which cannot be synthesized by CCSNe since the ^{56}Ni yields of CCSNe cannot exceed $\sim 4\,M_\odot$ (Umeda & Nomoto 2008). Supposing that the LCs of SLSNe are powered by ^{56}Ni, a novel method to solving this problem is supposing that the explosions are so-called “pair instability SNe” (PISNe) (Barkat et al. 1967; Rakavy & Shaviv 1967; Heger & Woosley 2002; Heger et al. 2003). For example, Gal-Yam et al. (2009) suggested that SN 2007bi is a PISN; Cooke et al. (2012) studied two high-redshift SLSNe and concluded that these two SLSNe might be PISNe.

2.1.1 Fast-evolving SLSNe I

Fast-evolving SLSNe I which constitute a major fraction of SLSNe I cannot be explained by the ^{56}Ni models since the decline rates of most of them are larger than those of LCs produced by the ^{56}Ni model (e.g., Quimby et al. 2011). In other words, the ^{56}Ni masses inferred from the peak luminosities are significantly larger than those inferred from the late-time LCs (e.g., De Cia et al. 2018).

Moreover, for all fast-evolving SLSNe I, high peak luminosities require a huge amount of ^{56}Ni while narrow LCs indicate that the masses of the ejecta are relatively small. Inserra et al. (2013) and Nicholl et al. (2014) modeled some fast-evolving SLSNe I and found that the amount of ^{56}Ni is $5 - 30\,M_\odot$ and the masses of the ejecta are between several $M_\odot$ to 30 $M_\odot$, therefore the ratios of required masses of ^{56}Ni to the ejecta masses are usually $\gtrsim$50% or even 100%, significantly larger than the upper limit ($\sim$20%, Umeda & Nomoto 2008) of the ratio of the ^{56}Ni mass to the ejecta mass.

These studies demonstrated that the ^{56}Ni models (including the CCSN model and PISN model) cannot account for fast-evolving SLSNe I.

2.1.2 Slowly-evolving SLSNe I

Only very few SLSNe I have slowly-evolving post-maximum LCs mimicking those of SNe powered by radioactive elements (mainly ^{56}Ni) which might be PISNe (Gal-Yam et al. 2009; Cooke et al. 2012), whose ^{56}Ni masses and ejecta masses can be $\gtrsim 5\,M_\odot$ and $100 - 110\,M_\odot$, respectively. Gal-Yam (2012) proposed that they belong to a distinct class whose energy source is radioactive elements and named this class “SLSNe R.”

However, Dessart et al. (2012) argued that SN 2007bi was not a PISN since its spectra are not consistent with those reproduced by PISN models. Alternatively, Dessart et al. (2012) suggested that SN 2007bi was powered by a magnetar. Moreover, Inserra et al. (2017) found that the decline rates of the LCs at $t - t_{\rm peak} \gtrsim 150$ d of four slowly-evolving SLSNe I (SN 2007bi, PTF12dam, SN 2015bn and LSQ14an) are inconsistent with those of LCs reproduced by ^{56}Co decay, indicating that they cannot be explained by the PISN model since the ejecta masses of PISNe are very large so that the decline rates of their LCs must be consistent with those of the ^{56}Co decay rate at $t - t_{\rm peak} \lesssim 500\,$d.

2.1.3 SLSNe II

Studies targeting some type II SLSNe, e.g., SN 2006gy (Agnoletto et al. 2009) and CSS121015 (Inserra et al. 2013), also demonstrated that the LCs of SLSNe II cannot be explained by both the normal ^{56}Ni model and the PISN model.

In summary, to date, only a small fraction of SLSNe might be powered by the decay of ^{56}Ni that was synthesized by PISNe. Most SLSNe cannot be explained by ^{56}Ni and must be accounted for by other models.

2.2 The Magnetar Model

CCSN explosions may leave behind fast-rotating neutron stars whose initial rotational periods (P_0) are several milliseconds to several seconds. Based on the observations of some SN remnants (SNRs), Ostriker & Gunn (1971) proposed that neutron stars with magnetic field strength $B \sim 10^{12}\,$G can play a key role in energizing both SNe and SNRs by injecting their rotational energy to the ejecta or shells.

The same model has been applied for modeling gamma-ray burst (GRB) prompt emission (Usov 1992; Metzger et al. 2007; Bucciantini et al. 2008; Metzger et al. 2011) and GRB afterglows (e.g., Dai & Lu 1998a,b; Zhang & Mészáros 2001; Dai 2004; Dai & Liu 2012). In these models, the neutron stars are highly magnetized, $B \sim 10^{14} - 10^{15}\,$G, and are called "magnetars."

The magnetar spinning-down model had also been introduced to study SNe. To account for the LC of SN 2005bf, which is not very luminous but cannot be explained by the ^{56}Ni model, Maeda et al. (2007) suggested that the energy source powering it is a newly-born magnetar and the initial spin period is $\sim$10 ms. Woosley (2010) and Kasen & Bildsten (2010) suggested that LCs of SLSNe can be powered by spinning-down magnetars whose initial spin periods and magnetic strength are $\sim 1 - 5\,$ms and $\sim 10^{14} - 10^{15}\,$G, respectively[2].

The shapes and peak luminosities of the LCs powered by magnetars depend sensitively on the values of κ, $M_{\rm ej}$, $v_{\rm sc}$, B and P_0. Supposing $\kappa = 0.1\,{\rm cm^2\,g^{-1}}$, $v_{\rm sc} = 10^9\,{\rm cm\,s^{-1}}$, $M_{\rm ej} = 10\,M_\odot$, κ_γ = infinity (full trapping), and setting $B_{14} = B/10^{14}{\rm G} = 5, 8, 10$ and $P_0 = 20, 5, 1.5\,$ms, we plot nine LCs powered by magnetars in Figure 2. Adopting this set of parameters, Figure 2 shows that the magnetar model can reasonably explain normal SNe, luminous SNe as well as SLSNe. If we fix the values of B and P_0 and vary the values of κ, $M_{\rm ej}$ and $v_{\rm sc}$, we can also get different LCs. Like the ^{56}Ni model, larger $M_{\rm ej}$ and κ or lower $v_{\rm sc}$ would result in dimmer peaks and broad LCs.

Inserra et al. (2013), Nicholl et al. (2013) and Nicholl et al. (2014) used the magnetar model with full trapping of high energy photons (gamma rays and X-rays) to fit the LCs of some SLSNe I and found that the LCs reproduced by this model are in good agreement with the observational data. As mentioned above, the model adopted by these groups was derived on the assumption of full-trapping of the gamma-ray and X-ray emission. When the hard emission was mainly X-ray emission, this assumption is valid and the LCs reproduced by this model can be in good/excellent agreement with observations. If the high-energy emission was dominated by gamma-ray emission, a fraction of hard emission would leak from the ejecta before softening to UV−optical−IR photons. Therefore, some LCs reproduced by the model with the assumption have tails brighter than the observation (Nicholl et al. 2014; Chen et al. 2015).

To solve this problem, Wang et al. (2015b) incorporated the leakage effect into the original magnetar-powered model. If the magnetar emission is dominated by gamma-ray ($E_\gamma \gtrsim 10^6\,$eV), $\kappa_\gamma \simeq 0.01 - 0.2\,{\rm cm^2\,g^{-1}}$; if the emission is dominated by X-ray ($10^2\,{\rm eV} \lesssim E_{\rm X} \lesssim 10^6\,$eV), $\kappa_{\rm X} \simeq 0.2 - 10^4\,{\rm cm^2\,g^{-1}}$, (see fig. 8 of Kotera et al. 2013). By analyzing the late-time LC of PTF12dam, Chen et al. (2015) also found the magnetar model with full trapping cannot fit the late-time LC of PTF12dam and introduced a similar trapping factor. Using this revised magnetar-powered model, the SLSNe whose LC tails cannot be fitted by the magnetar model with full trapping were explained well, see, e.g., Figure 3.

Although Woosley (2010) and Kasen & Bildsten (2010) had demonstrated that the acceleration effect is rather notable, the models based on Arnett (1982) all neglect acceleration of the SN ejecta caused by magnetar wind. Besides, the photospheric recession effect is also omitted in these models. Wang et al. (2016b) proposed a new semi-analytic magnetar-powered model that has taken these two effects into account. In this new magnetar-powered model, the photospheric velocity of an SLSN is smaller than the scale velocity $v_{\rm sc}$ and its evolution must be fit. Moreover, the scale velocity itself is a running quantity

[2] Wang et al. (2016a, 2017a,c) and Chen et al. 2017 demonstrated that the LCs of some broad-lined SNe Ic might be powered by millisecond magnetars if the magnetic strength of these putative magnetars is a few $10^{16}\,$G.

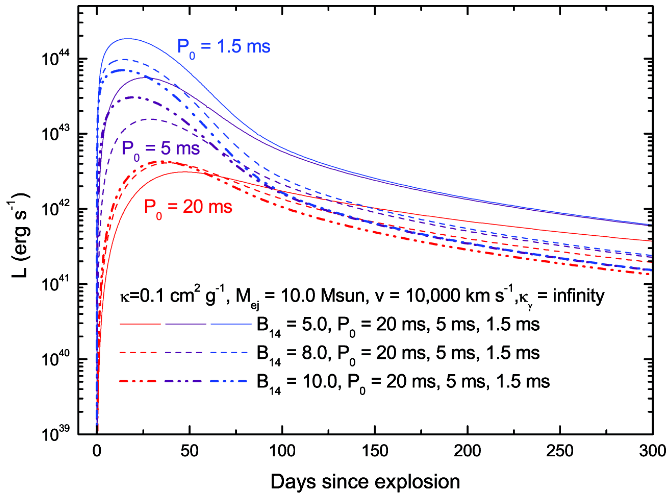

Fig. 2 LCs powered by magnetar model. We fix $\kappa = 0.1\,\mathrm{cm^2\,g^{-1}}$, $M_{\rm ej} = 10\,M_\odot$ and $v_{\rm sc} = 10^9\,\mathrm{cm\,s^{-1}}$. The LCs powered by magnetars with the same initial rotational periods are presented by the same colors.

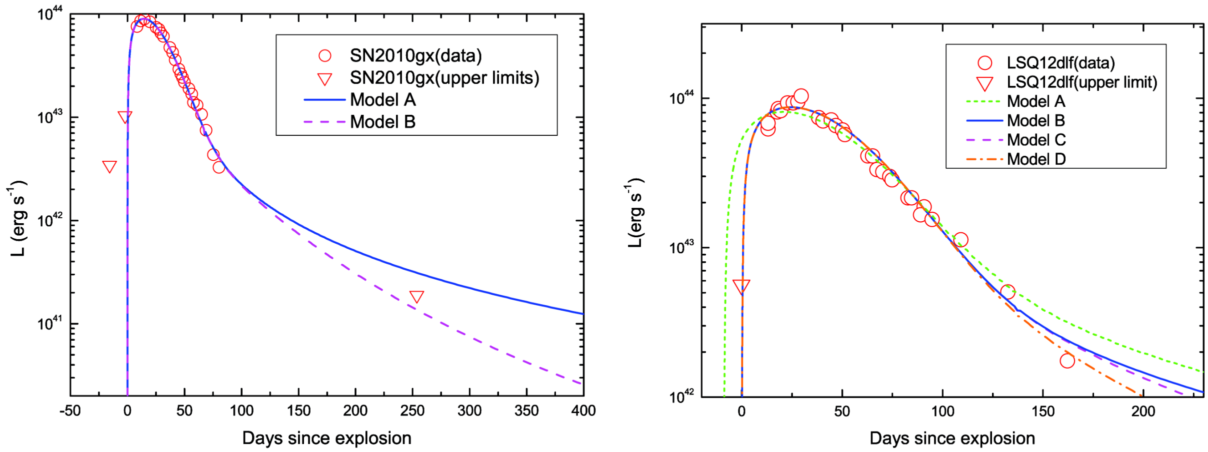

Fig. 3 LCs in the original magnetar-powered model and the revised magnetar-powered model for SN 2010gx and LSQ12dlf. The *solid lines* and *dashed lines* are produced by the magnetar models without and with leakage effect, respectively (Wang et al. 2015b).

and is not a parameter or a measurable quantity. Instead, the initial scale velocity $v_{\rm sc0}$ is a free parameter.

Using this model, Liu et al. (2017a) fitted the data of 19 SLSNe I and found that the LCs, temperature evolution and photometric velocity evolution reproduced by this model are in good agreement with the observations and $\sim 19\% - 97\%$ of initial rotational energy of the magnetars was converted to kinetic energy of the ejecta (Nicholl et al. (2017c) and Yu et al. (2017) also used the magnetar model to fit the multi-band LCs or bolometric LCs of dozens of SLSN I and got satisfactory results.). Moreover, they found that the initial kinetic energies of most of these SLSNe are smaller than $\sim 2 \times 10^{51}$ erg which is the upper limit of the kinetic energies that can be provided by the neutrino-powered mechanism (Ugliano et al. 2012; Janka 2012; Sukhbold et al. 2016).

Soker & Gilkis (2017) investigated 38 SLSNe I discovered by the Pan-STARRS1 medium deep survey (PS1 MDS, Lunnan et al. 2018) and suggested that the SLSNe which are supposed to be powered by magnetars should be firstly powered by jets launched from the surfaces of the magnetars. Further investigations into the magnetar model are needed.

For an SLSN that can be explained by a magnetar, the contribution from ^{56}Ni can be neglected since an SLSN leaving a magnetar is a CCSN whose ^{56}Ni yield is usually rather low, $\lesssim 0.2\,M_\odot$, and the luminosity from this amount of ^{56}Ni is significantly smaller than that of an SLSN (Inserra et al. 2013).

2.3 The Ejecta-CSM Interaction Model

Before the explosions, the progenitors of SNe are surrounded by circumstellar winds or material shells ejected from progenitors just prior to the SN explosions. After the explosions, the SN ejecta collides with the winds or shells, generating forward shocks and reverse shocks whose dynamics can be described by self-similar solutions (Chevalier 1982; Chevalier & Fransson 1994). In some extreme cases, the "pulsational pair-instability (PPI)" mechanism (Heger et al. 2003; Woosley et al. 2007; Pastorello et al. 2008; Chugai 2009; Chatzopoulos & Wheeler 2012) might expel some shells in different epochs; faster shells might catch up and collide with the slower shells, also generating forward shocks and reverse shocks. The shock-accelerated electrons emit gamma- and X-ray photons and most of these photons would be softened to UV$-$optical$-$IR photons. These processes convert the kinetic energy of the ejecta or the faster shells to radiative energy of the SNe and might significantly increase the luminosities of some SNe if the density of circumstellar wind or shells is high enough.

The LCs of SLSNe IIn cannot be explained by any model neglecting the contributions from interaction-induced shocks. In fact, the ejecta-CSM interaction model in which the LCs of these SNe are powered by interaction between the SN ejecta and the hydrogen-rich (and hydrogen-poor) CSM is the most natural model explaining SNe IIn (e.g., Chugai & Danziger 1994; Miller et al. 2010; Zhang et al. 2012), Ibn (e.g., Chugai 2009) as well as SLSNe IIn (e.g., Smith & McCray 2007; Moriya et al. 2013; Nicholl et al. 2014). Since the properties of CSM are very complicated, the LCs of luminous SNe IIn, Ibn and SLSNe IIn aided by the ejecta-CSM interaction show great complexity (see Smith 2017 and references therein).

Many studies have demonstrated that the LCs of SLSNe I and SLSNe IIL whose spectra lack narrow lines, indicative of ejecta-CSM interactions or shell-shell interactions, can be explained by the magnetar-powered model. Although the absence of the interaction signatures in the spectra of SLSNe I and IIL indicates that the contributions from the interactions can be neglected in explaining these two classes of SLSNe, the possibility that these SLSNe are powered by interactions cannot be excluded since the interaction is not necessary to prompt corresponding signs (e.g., narrow and intermediate-width Hα emission lines).

Ginzburg & Balberg (2012) applied the interaction model to fit the LCs of SN 2010gx (type I) and SN 2006gy (type IIn). Nicholl et al. (2014) also used this semi-analytic model to fit some SLSNe I since the late-time LCs reproduced by the magnetar-powered model neglecting late-time leakage are inconsistent with observations. Tolstov et al. (2017) argue that PTF12dam (SLSN I) can be powered by shell-shell collision.

Recently, Liu et al. (2018) constructed an ejecta–CSM interaction model involving multiple interactions between the ejecta and different shells/winds and fit the LCs of iPTF13edcc and iPTF15esb, see Figure 4.

2.4 The Fallback (Jet-Ejecta Interaction) Model

The collapsar model (Woosley 1993; MacFadyen & Woosley 1999) for GRBs proposes that a black hole-disk system can launch a relativistic jet which can punch a hole in the mantle of a stripped progenitor and produce gamma ray emission. In this model, the Fe core collapses to a black hole and the inner mantle material with high angular momentum falls back and forms an accretion disk.

If the jet cannot break out and is trapped by the stellar mantle, energy carried by the jet will be deposited and thermalized to black-body emission. Dexter & Kasen (2013) studied this possibility and found that this "failed" jet could significantly change the optical LC powered by the explosion. This model is a jet-ejecta interaction model and can be used to explain SN LCs with different peak luminosities and durations. Wang et al. (2018) explained the unusual type II-P SN iPTF14hls, which is not an SLSN, as episodic fallback accretion onto a neutron star. If the deposited energy is large, this model can power a peak luminosity $\gtrsim 10^{44}\,\mathrm{erg\,s^{-1}}$ and reproduce the LCs of SLSNe I and II. Gao et al. (2016) used a similar model to explain ultra-long GRB 111209A and associated SN (SN 2011kl).

Moriya et al. (2018) used the fallback model to fit 37 SLSNe I and found that the LCs produced by this model can be consistent with observations. Moreover, they adopted a typical conversion efficiency 10^{-3} and estimated the required total energy of the accretion disk, finding that the inferred mass of the accretion disk is $2-700\,M_{\odot}$. They concluded that only a fraction of SLSNe I whose rising timescales are relatively short ($\lesssim 40\,\mathrm{d}$) can be explained by this model, or the conversion efficiency must be significantly larger than 10^{-3}. As pointed out by Moriya et al. (2018), it is difficult to distinguish the magnetar model from the fallback model using the LCs produced by these two models.

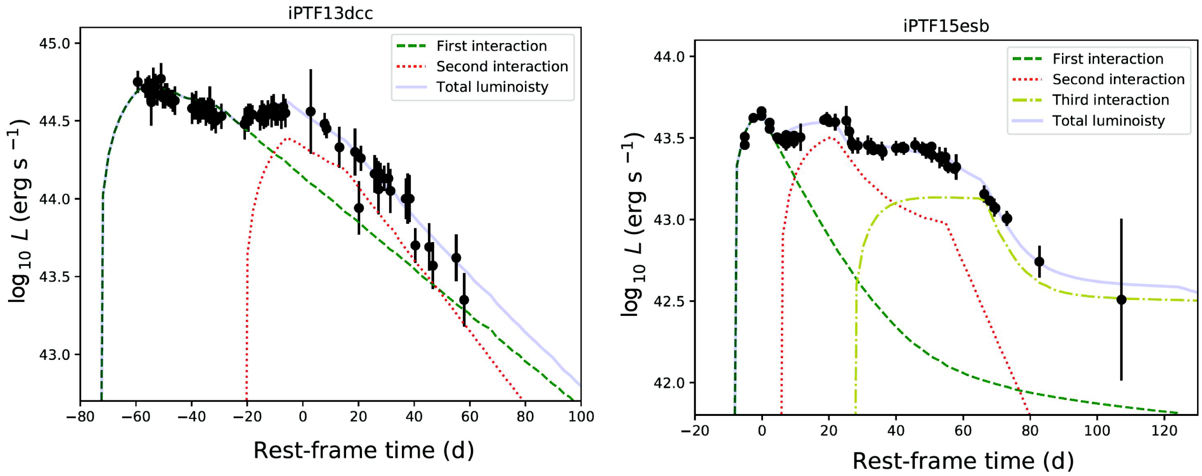

Fig. 4 The bolometric LCs of iPTF13edcc and iPTF15esb and the LCs reproduced by the multiple interaction model (Liu et al. 2018).

3 DOUBLE ENERGY-SOURCE MODELS

3.1 Cooling plus ^{56}Ni/Magnetar/Interaction Models

After the SN explosion, an energetic shock must be launched from the center of the SN and the shock-breakout (see Waxman & Katz 2017 and references therein) marked by the UV (for non-relativistic shock breakout) or X-ray/gamma-ray (for relativistic shock breakout) emission would appear, and the envelope would be heated to a temperature of millions of Kelvin (K). If the progenitors of SNe/SLSNe have extended envelopes, the cooling emission from shock-heated envelopes would power an LC whose initial luminosity can reach $\gtrsim 10^{42}\,\mathrm{erg\,s^{-1}}$. The cooling emission from a shock-heated envelope usually peaks at the UV$-$optical band and its duration is usually very short, $\sim$ a few days.

Piro (2015) proposed a concise model that can describe the behavior of the LC and temperature evolution powered by the cooling emission. The free parameters of this model are the optical opacity (κ), mass (M_e) and the initial radius (R_e) of the extended envelope, the mass of the core of the SN (M_c), as well as the kinetic energy of the SN (E_sn). The LC plotted in Figure 5 is yielded by a shock-heated extended envelope model with $\kappa = 0.1\,\mathrm{cm^2\,g^{-1}}$, $M_\mathrm{e} = 0.4\,M_\odot$, $R_\mathrm{e} = 500\,R_\odot$, $M_c = 5\,M_\odot$ and $E_\mathrm{sn} = 6.75 \times 10^{51}$ erg.

SLSNe having double-peaked LCs have been observed, e.g., LSQ14bdq (Nicholl et al. 2015), DES14X3taz (Smith et al. 2016), PTF12dam (Vreeswijk et al. 2017), SN 2006oz (Leloudas et al. 2012; Nicholl & Smartt 2016) and PS1-10pm (McCrum et al. 2015). Many groups (Nicholl et al. 2015; Smith et al. 2016; Vreeswijk et al. 2017; Nicholl & Smartt 2016) suggested that the first peaks of LCs for these SLSNe were powered by the cooling emission from the shock-heated extended envelopes and the second peaks (main peaks) might be powered by magnetars or ejecta-CSM interactions. In this model, the cooling emission powers the first peak and ^{56}Ni synthesized in the shock-heated ejecta or the magnetar left by the explosion or the interaction between the ejecta and the CSM would provide energy for the second peak and late-time decay. Energy released by other processes would quickly outshine the cooling emission and shape the second LC peak. Figure 6 shows an LC powered by the cooling emission and a magnetar.

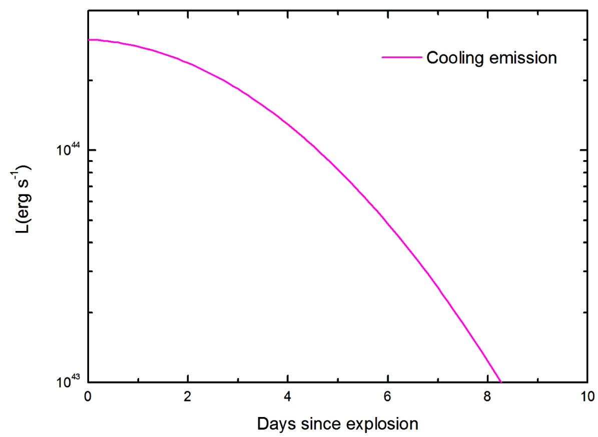

Fig. 5 LC powered by cooling emission from a shock-heated envelope, parameters can be found in the text.

For the SLSNe whose first peaks were missed by observations or only have single peaks, cooling emission can be neglected and their whole LCs might be powered by ^{56}Ni/magnetar/interaction (see Subsect. 2.1, 2.2 and 2.3) or their combinations (see below).

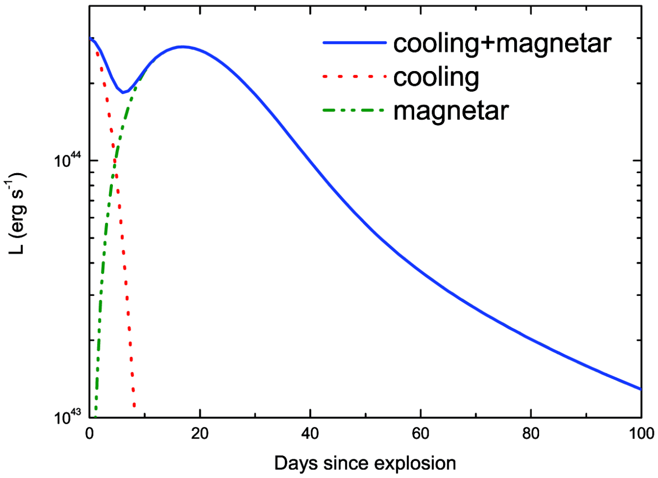

Fig. 6 The LCs produced by the cooling model, the magnetar model and the cooling plus magnetar model. $\kappa = 0.1\,\mathrm{cm^2\,g^{-1}}$, $M_\mathrm{e} = 0.4\,M_\odot$, $R_\mathrm{e} = 500\,R_\odot$, $M_\mathrm{c} = 5\,M_\odot$, $E_\mathrm{sn} = 6.75 \times 10^{51}$ erg, $v = 1.5 \times 10^9\,\mathrm{cm\,s^{-1}}$, $B = 3 \times 10^{14}$ G and $P_0 = 3$ ms.

3.2 The Magnetar plus ^{56}Ni Model

As mentioned above, the contribution from ^{56}Ni cascade decay is significantly smaller than that from other energy sources (magnetar or interaction) and can be neglected in modeling for SLSNe. However, the magnetar model and interaction model cannot explain Fe lines (if observed) in the spectra, and a moderate amount of ^{56}Ni is needed to explain the Fe lines related to ^{56}Ni.

Some luminous SNe whose peak magnitudes are between ~ -20 mag and -21 mag (e.g., Deustua et al. 1995; Schmidt et al. 2000; Howell et al. 2006; Sanders et al. 2012; Taddia et al. 2015; Greiner et al. 2015; Roy et al. 2016; Arcavi et al. 2016; Inserra et al. 2018) were also discovered in the past two decades.[3] Wang et al. (2015a) studied three luminous SNe Ic-BL and found that they cannot be explained by the ^{56}Ni model.

To solve these two problems, Wang et al. (2015a) proposed that luminous SNe Ic can also be powered by nascent magnetars whose initial rotational periods (P_0) are ~ 10 ms. Furthermore, Wang et al. (2015a) suggested that the contribution from some amount of ^{56}Ni cannot be omitted since the luminous SNe are not as bright as SLSNe. Therefore, they proposed that these SNe might be powered by magnetars with $P_0 \sim 10$ ms and $\sim 0.1 - 0.2\,M_\odot$ of ^{56}Ni. Bersten et al. (2016), Metzger et al. (2015) and Wang et al. (2017d) also employed the double energy sources (magnetar + ^{56}Ni) to fit the most luminous GRB-SN, SN 2011kl.

[3] Although some authors (e.g., Bersten et al. 2016; Inserra et al. 2018) regarded these luminous SNe as SLSNe, we still adopt the "ridgeline" ($M_\mathrm{peak} = -21$ mag) given by Gal-Yam (2012) and suggest that these luminous SNe belong to a class of " gap-filler" events that bridge ordinary SNe and SLSNe (Wang et al. 2015a; Arcavi et al. 2016).

Recently, Blanchard et al. (2019) studied the multi-band LC and spectra of SN 2017dwh which is an SLSN I that exploded at $z \approx 0.13$. Based on the post-peak spectra showing a strong absorption line centered near 3200 Å which is inferred to be Co II and the late-time spectra which also provide evidence for the existence of a large mass of Fe-group elements, Blanchard et al. (2019) concluded that this SLSN synthesized $\lesssim 0.6\,M_\odot$ and used a magnetar plus ^{56}Ni model to model the multi-band LC and obtained a rather good result. Blanchard et al. (2019) found that the best-fitting parameter of ^{56}Ni is $0.89^{+0.52}_{-0.58}\,M_\odot$ (1σ confidence) whose lower limit ($0.31\,M_\odot$) is consistent with the lower limit ($\lesssim 0.6\,M_\odot$) inferred from the spectra.

Based on these studies, we can conclude that some luminous SNe and SLSNe can be explained by the magnetar plus ^{56}Ni model.

3.3 The Interaction plus ^{56}Ni/Magnetar/Fallback Model

To fit the LC of SN 2006gy, Smith & McCray (2007) constructed a double-energy model containing the contributions from shock-heated material and ^{56}Ni cascade decay. This is the ejecta-CSM interaction plus ^{56}Ni model. In this model, the photons coming from shock-heated ejecta and CSM powered the peak-luminosity as well as the early LC while the late-time LC was powered by $8\,M_\odot$ of ^{56}Ni. To synthesize this great amount ($8\,M_\odot$) of ^{56}Ni, the explosion must be a PISN.

Chatzopoulos et al. (2012) found that the LC of SN 2006gy can be explained by the ejecta-CSM interaction plus $2\,M_\odot$ of ^{56}Ni. The inferred ^{56}Ni mass is significantly smaller than that inferred by Smith & McCray

(2007). The ejecta mass derived by Chatzopoulos et al. (2012) is 40 $M_\odot$, indicating that if this result is correct, SN 2006gy is a CCSN rather than a PISN since the final masses (ejecta masses) of PISNe must be $\gtrsim 80\, M_\odot$ (see, e.g., Chatzopoulos et al. 2013a). However, how a CCSN can synthesize 2 $M_\odot$ of ^{56}Ni is still a puzzle. Besides, Chatzopoulos et al. 2013b used the interaction plus ^{56}Ni model to fit 12 SLSNe (five SLSNe I and seven SLSNe II) and got rather good results (they also adopted other models to fit the LCs of these SLSNe).

To fit the LC of the type Ic SN iPTF16asu whose rise time is as short as four days in the rest frame, Wang et al. (2017b) constructed a model including early interaction and late-time energy input from a magnetar. Chen et al. (2018) adopted the interaction plus magnetar model as well as fallback + interaction model to fit the bolometric LC of SLSN 2017ens.

4 TRIPLE ENERGY-SOURCE MODEL

Yan et al. (2015) studied a type I SLSN, iPTF13ehe, and suggested that its nebula spectra indicate 2.5 $M_\odot$ of ^{56}Ni. If this SLSN was powered by ^{56}Ni, however, the required ^{56}Ni would be $\gtrsim 13 - 16\, M_\odot$, significantly larger than the value inferred from the spectral analysis. These facts indicate that the LC of iPTF13ehe cannot be explained by the ^{56}Ni model. Wang et al. (2016c) modeled this SLSN using a magnetar model and magnetar plus ^{56}Ni model, and found both these two models can reproduce the early-time LC of this SLSN.

Since the late-time spectrum shows narrow Hα emission lines indicative of ejecta-CSM interaction and the late-time LC has a brightening feature, Yan et al. (2015) proposed that the ejecta-CSM interaction was triggered when the ejecta collided with the hydrogen-rich CSM shell expelled prior to the explosion and produced late-time brightening as well as Hα emission lines. Wang et al. (2016c) developed a triple energy-source model containing the contributions from ^{56}Ni, magnetar and ejecta-CSM interaction to reproduce the LC of iPTF13ehe; see Figure 8.

Yan et al. (2015) estimated that $\sim$15% of SLSNe I might have late-time Hα emission lines. Obviously, these SLSNe can be explained by double (magnetar plus interaction) or triple energy-source models (^{56}Ni plus magnetar plus interaction).

The models containing cooling emission from the shock-heated envelopes of the SN progenitors and the combinations of ^{56}Ni+magnetar or ^{56}Ni+interaction or magnetar+interaction are also triple energy-source models. To account for the LC of SN 2011kl which is a luminous type Ic SN, Wang et al. (2017d) employed the cooling+^{56}Ni+magnetar model.

5 DISCUSSION

5.1 The Validity of the Models

Determining the energy sources of SLSNe is very difficult, but the energy sources should leave their imprints on the SLSN LCs and spectra. For example, if an SLSN is powered by a newly-born magnetar, the magnetar wind would sweep a shell surrounding a bubble. Then the spectra would show a velocity plateau (Kasen & Bildsten 2010). If an SLSN is powered by the interaction between the ejecta and CSM, there might be some narrow emission lines in their spectra. If these narrow Hα emission lines are discovered in the spectra of all SNe IIn and SLSNe IIn, then the interaction model is valid for explaining SNe IIn and SLSNe IIn. However, as pointed out by Liu et al. (2017b), no narrow emission lines are found in the spectra of 32 SLSNe I collected by them, indicating that these SLSNe might not be powered by the interaction. Nevertheless, interactions do not prompt emission lines if the temperature and/or density of the CSM is low. Therefore, the interaction model cannot be ruled out.

To test the one-dimensional magnetar model, Liu et al. (2017b) analyzed the photospheric velocity evolutions of 13 SLSNe. They found that only two SLSNe I (PTF10hgi and PS1–11ap) show slow velocity-evolution features that are consistent with the one-dimensional magnetar model and the velocity evolution of the other 11 SLSNe is fast, indicating that the spectra of most SLSNe cannot be explained by the one-dimensional magnetar model. However, the two-dimensional magnetar model (Chen et al. 2016) can destroy the shell structure and the spectra might quickly evolve.

By studying the spectra of SN 2015bn, Nicholl et al. (2016b) suggest that the strong and relatively narrow O I λ 7774 line may indicate the existence of an inner shell swept by a central engine. Furthermore, they argue that the putative central engine might be a magnetar, rather than a black hole. Based on 1000 d of photometric observations targeting SN 2015bn, Nicholl et al. (2018) find that the LC at very late epoch is consistent with $L \propto t^{-4}$ which can be yielded by a magnetar spin-down input with inefficient gamma-ray trapping and pointed out that this LC feature indicates the existence of a nascent magnetar.

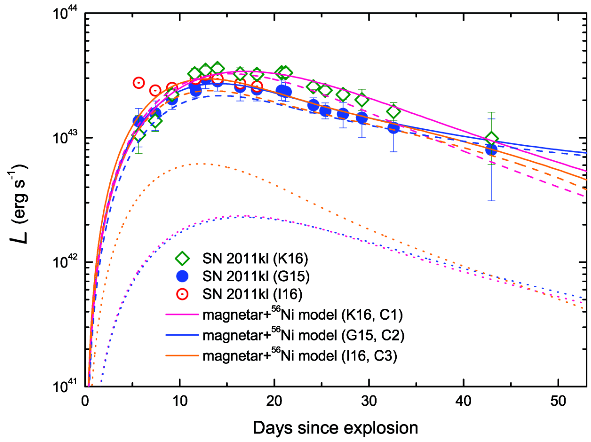

Fig. 7 The magnetar + ^{56}Ni model (*solid lines*) for the LC of SN 2011kl (Wang et al. 2017d). The *dotted lines* represent the LCs reproduced by 0.1 (the dimmer LCs) or 0.2 M$\odot$ (the brighter LCs) of ^{56}Ni; the *dashed lines* signify the LCs powered by magnetars.

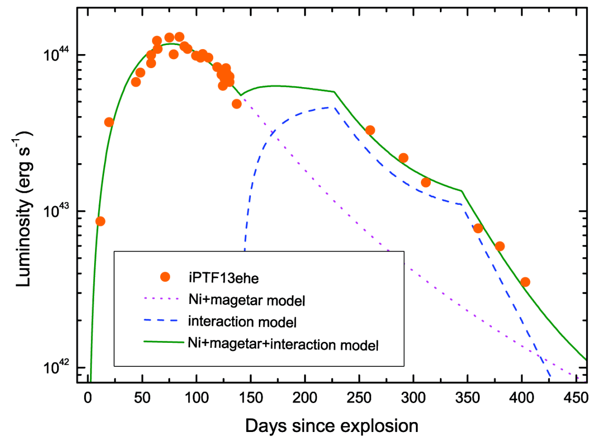

Fig. 8 Modeling LC of iPTF13ehe using the triple-energy model (^{56}Ni + magnetar + interaction) (Wang et al. 2016c).

5.2 The Explosion Mechanisms of SLSNe and Luminous SNe

It is believed that SNe Ia, Iax and Ia-CSM might originate from the explosions of white dwarfs, and that other subclasses of normal-luminosity SNe are CCSNe. In contrast, the explosion mechanisms of SLSNe and luminous SNe are still elusive.

It seems that almost all SLSNe II and fast-evolving SLSNe I ever discovered might have originated from the explosions of CCSNe. However, the explosion mechanisms of slowly-evolving SLSNe I are still elusive. Nicholl et al. (2013) modeled the LC of rapidly-rising, slowly-declining SLSN PTF12dam and analyzed its spectra, concluding that this SLSN cannot be explained by the ^{56}Ni-powered model since the rise time of the LC produced by the ^{56}Ni synthesized by PISNe is larger than that of the observed LC. It should be mentioned that Kozyreva & Blinnikov (2015) proposed a PISN model in which ^{56}Ni is strongly mixed into ejecta and the rise time of LCs produced by this PISN model is short enough to fit the observational data. As pointed out by Moriya et al. (2017), however, strong ^{56}Ni mixing has not yet been discovered by multidimensional PISN simulations.

5.3 The Progenitors of SLSNe

In the past decades, the progenitors of dozens of SNe have been confirmed directly (see Smartt 2009 and references therein). Unfortunately, none of these SNe is an SLSN since all progenitors of SLSNe are too distant ($z \gtrsim 0.1$) to be detected before their explosions.

However, many lines of evidence indicate that the progenitors of SLSNe might be massive stars. The first piece of evidence is that the explosions of white dwarfs cannot produce such bright transients even if the white dwarfs are "super-Chandrasekar" ones. The second piece of evidence is that the spectra of most SLSNe resemble normal-luminosity CCSNe produced by the explosions of massive stars. The third piece of evidence is that most SLSNe are located in star-forming dwarf galaxies[4].

Almost all SLSNe are located in low-metallicity dwarf galaxies[5], suggesting that the metallicities of the progenitors of SLSNe are rather low. A massive star with low-metallicity has very low mass-loss rate. However, the progenitor of an SLSN I must have lost its hydrogen envelope or even the helium envelope. Therefore, it can be expected that the progenitors of SLSNe I might be in binary systems and the envelopes of these progenitors must be stripped by their companions. This mechanism involving mass transfer has another advantage that the striping process can spin-up the progenitors and is beneficial for the formations of millisecond magnetars which might power the LCs of SLSNe.

[4] For example, the SFR of the host galaxy of PS1-10bzj is $2-3\,M_\odot\,\mathrm{yr}^{-1}$. Since the mass of this host galaxy is $\approx 2.4\times10^7\,M_\odot$, its specific SFR (sSFR) is $\approx 10^{-7}\,\mathrm{yr}^{-1} = 10^2\,\mathrm{Gyr}^{-1}$ (Lunnan et al. 2013). Using the high angular-resolution UV imaging obtained by *HST*, Lunnan et al. (2015) studied the morphological properties, sizes and SFR densities of the host galaxies of 16 SLSNe I and found that these galaxies are compact, irregular galaxies and their UV-derived SFR densities are high (the averaged value is $\simeq 0.1\,M_\odot\,\mathrm{yr}^{-1}\,\mathrm{kpc}^{-2}$, Lunnan et al. 2015).

[5] For example, the metallicity of the host galaxies of SN 2007bi, PS1-10bzj and SN 2010gx are 1/3 $Z_\odot$ (Young et al. 2010), 0.1 $Z_\odot$ (Lunnan et al. 2013) and 0.06 $Z_\odot$ (Chen et al. 2013), respectively.

5.4 SLSN-GRB Connection

A minor fraction of SNe Ic have spectra with very broad absorption troughs which indicate very large photospheric velocities and are named broad-lined SNe Ic (SNe Ic-BL) (Woosley & Bloom 2006). Some SNe Ic-BL associated with long GRBs have been discovered just after the detections of the corresponding GRBs (Galama et al. 1998; Stanek et al. 2003; Hjorth et al. 2003; Gal-Yam et al. 2004; Campana et al. 2006; Mazzali et al. 2006; Berger et al. 2011; Starling et al. 2011; Melandri et al. 2012; Xu et al. 2013; Cano et al. 2014, 2015; D'Elia et al. 2015; Toy et al. 2016; Ashall et al. 2017; Cano et al. 2017b; see Woosley & Bloom 2006; Hjorth & Bloom 2012; Cano et al. 2017a for reviews).

The SNe associated with GRBs are dimmer than SLSNe. To date, the most luminous GRB-SN might be SN 2011kl whose peak bolometric magnitude is $\simeq -20.25 \pm 0.06$ mag (Kann et al. 2016) while the peak bolometric magnitudes of SLSNe are $\lesssim -21$ mag. However, the nature of SN 2011kl is still under debate. Greiner et al. (2015) suggest that it is an SN while Ioka et al. (2016) argue that it might be a TDE. If SN 2011kl is a TDE, the peak bolometric magnitude of the most luminous GRB-SN is $\gtrsim -19$ mag.

Matsumoto et al. (2016) investigated the model supposing that the jet successfully breaks out and generates a GRB while the forward and reverse shocks produced will shock the envelope material and form a hot cocoon. Matsumoto et al. (2016) calculated the cocoon emission associated with the black hole-disk system produced by supermassive population III stars whose masses are $\sim 10^5\, M_\odot$ at high redshift ($z \gtrsim 6$) and found that the jet cocoons will significantly enhance the optical luminosities of the SNe associated with the GRBs and predicted that the jet–cocoon emission will power very luminous SNe whose peak luminosities are $\sim 10^{45} - 10^{46}\,\mathrm{erg\,s^{-1}}$ (the corresponding peak bolometric magnitudes are $\simeq -24$ mag to $\simeq -26$ mag) after the cocoon breaks out of the envelopes. While these high-redshift, superluminous GRB-SLSNe have not yet been discovered, Matsumoto et al. (2016) expect that they will be detected by upcoming NIR telescopes.

5.5 SLSNe vs. Tidal Disruption Events

Judging whether a superluminous optical transient is an SLSN is rather challenging. As pointed out by Quimby et al. (2013), it is very difficult to distinguish between active galactic nuclei (AGNs), tidal disruption events (TDEs) and SLSNe even if we have multi-band photometry, spectra and high resolution images.

For example, Vinkó et al. (2015) demonstrated that the very luminous ($L_{\rm peak} > 5 \times 10^{44}\,\mathrm{erg\,s^{-1}}$) optical transient *Dougie* might be a super-Eddington TDE, rather than an SLSN; Dong et al. (2016) suggested that ASASSN-15lh is the most luminous SN discovered so far while Leloudas et al. (2016) argued that it is a TDE.

Although modeling these luminous optical transients would help to determine their nature, comprehensive observations of their multi-band LCs and multi-epoch spectra are also needed.

6 CONCLUSIONS

In the past two decades, SLSNe whose peak luminosities are $\gtrsim 7 \times 10^{43}\,\mathrm{erg\,s^{-1}}$ have been discovered by many sky-survey telescopes, and the efforts to unveil the energy sources and nature of SLSNe have been done by many groups. The LCs and spectra of SLSNe are rather heterogeneous, reflecting the diverse physical parameters, e.g., energies, ejecta masses, ejecta velocities and some other parameters associated with their central remnants which might play key roles in powering their LCs. Observing SLSNe and modeling their LCs offer new opportunities to study the evolution and explosion mechanisms of massive stars.

In this *review*, we present five single energy-source models which have been used to explain the LCs of SLSNe (and normal SNe), i.e., the ^{56}Ni cascade decay model, magnetar model, ejecta-CSM interaction model, fallback (jet-ejecta interaction) model, cooling model as well as their different combinations.

Unlike normal SNe whose LCs can be reasonably explained by the models mentioned above, it is much less clear how SLSNe can be powered by these plausible energy sources. The LCs of normal SNe are mainly powered by ^{56}Ni cascade decay and the role of neutron-star spinning-down and the ejecta-CSM interaction can be neglected in the modeling for most SNe, except for types IIn, Ibn and Ia-CSM SNe. On the other hand, accumulating observational data and theoretical modeling indicate that the ^{56}Ni model cannot account for most of the LCs of SLSNe and luminous SNe since this scenario requires a huge amount of ^{56}Ni inside the ejecta to account for their peak luminosities and the fact that the energy from nascent magnetars or ejecta-CSM interaction can play an essential role in powering the LCs of a majority of SLSNe and luminous SNe. However, we cannot conclude that these SLSNe must be powered by magnetars or ejecta-CSM interaction and cannot discriminate between these two models even if the LCs of SLSNe can be explained by one or both of these two models. To account for the complicated LCs of some SLSNe, the triple energy-source model might be employed.

The cooling emission from shock-heated envelopes of the progenitors would produce the first peaks of the LCs of some SLSNe having double-peaked LCs and the emission from ^{56}Ni or magnetar or ejecta-CSM interactions can power the second peaks. The first peaks might usually be missed due to the lack of very early observations for some SLSNe.

An appealing unified scenario is that type I SLSNe, type IIL SLSNe, luminous SNe Ic and normal SNe Ic are powered by neutron stars plus ^{56}Ni while type IIn SLSNe, luminous SNe IIn and normal SNe IIn are powered by the ejecta-CSM interaction plus ^{56}Ni. In this scenario, the ^{56}Ni masses are roughly constant ($\sim 0.1\,M_{\odot}$), and the difference of their neutron-star properties (the initial rotational periods P_0, the magnetic field strength B) or the ejecta and CSM properties (the ejecta mass, the ejecta velocity, the CSM mass, the CSM density profile and so on) result in different luminosity and rise/decline rate, while the ejecta masses and velocities determine the LC width.

Extreme conditions are required if these models are valid for explaining SLSNe. For SLSNe powered by ^{56}Ni, a huge amount ($\gtrsim 5\,M_{\odot}$) of ^{56}Ni must be synthesized and the SNe might be PISNe; For SLSNe powered by magnetars, magnetars with very short initial rotational periods ($P_0 \lesssim 10\,$ms) and very strong magnetic field strengths ($\gtrsim 10^{13}{-}10^{15}$ G) must be left after explosions and the SNe must be CCSNe; For SLSNe powered by ejecta-CSM interactions or shell-shell interactions, the progenitors might be η Carinae-like stars and must experience strong wind loss or (multiple) giant eruptions (just) prior to the explosions and the final explosions can be CCSNe or PISNe, depending on the ^{56}Ni masses required.

Although the most prevalent semi-analytic models can yield LCs that are in good agreement with the photometric observations, their disadvantages are obvious: neglecting the time- and space-dependent effect of optical opacity, the mixing effect and the two/three-dimensional effect. Besides, some very luminous optical transients having very bright peak luminosities (peak absolute magnitudes are $\lesssim -20.5\,$mag) and very short rising time scales ($\lesssim 10\,$d) cannot be explained well by any models mentioned above. More detailed modeling might provide more useful information and eventually determine their nature and their energy sources.

Determining the energy sources of SLSNe requires more dedicated observations and theoretical studies. Radio and X-ray observations for the remnants of some SLSNe also help us to judge whether or not the LCs of SLSNe are powered by magnetars or the ejecta-CSM interactions or other complicated models. New sky-survey programs (the Zwicky Transient Facility (ZTF), Law et al. 2009) and upcoming sky-survey programs (e.g., the Large Synoptic Survey Telescope (LSST), Ivezić et al. 2008; LSST Science Collaboration et al. 2009) should be able to discover more nearby SLSNe and intense follow-up photometric and spectral observations for them would shed more light on the nature of these optical transients. Modeling these SLSNe would help to determine their energy sources.

Acknowledgements We thank Weikang Zheng for helpful discussions. This work was supported by the National Key Research and Development Program of China (Grant No. 2017YFA0402600) and the National Natural Science Foundation of China (Grant Nos. 11573014 and 11833003).

References

Agnoletto, I., Benetti, S., Cappellaro, E., et al. 2009, ApJ, 691, 1348
Arcavi, I., Wolf, W. M., Howell, D. A., et al. 2016, ApJ, 819, 35
Arnett, W. D. 1982, ApJ, 253, 785
Ashall, C., Pian, E., Mazzali, P. A., et al. 2017, arXiv:1702.04339
Baade, W., & Zwicky, F. 1934, Physical Review, 46, 76
Barkat, Z., Rakavy, G., & Sack, N. 1967, Physical Review Letters, 18, 379
Berger, E., Chornock, R., Holmes, T. R., et al. 2011, ApJ, 743, 204
Bersten, M. C., Benvenuto, O. G., Orellana, M., & Nomoto, K. 2016, ApJ, 817, L8
Blanchard, P. K., Nicholl, M., Berger, E., et al. 2019, ApJ, 872, 90
Bose, S., Dong, S., Pastorello, A., et al. 2018, ApJ, 853, 57
Bucciantini, N., Quataert, E., Arons, J., Metzger, B. D., & Thompson, T. A. 2008, MNRAS, 383, L25
Campana, S., Mangano, V., Blustin, A. J., et al. 2006, Nature, 442, 1008
Cano, Z., de Ugarte Postigo, A., Pozanenko, A., et al. 2014, A&A, 568, A19
Cano, Z., de Ugarte Postigo, A., Perley, D., et al. 2015, MNRAS, 452, 1535
Cano, Z., Wang, S.-Q., Dai, Z.-G., & Wu, X.-F. 2017a, Advances in Astronomy, 2017, 8929054
Cano, Z., Izzo, L., de Ugarte Postigo, A., et al. 2017b, A&A, 605, A107
Cappellaro, E., Mazzali, P. A., Benetti, S., et al. 1997, A&A, 328, 203
Chatzopoulos, E., & Wheeler, J. C. 2012, ApJ, 760, 154
Chatzopoulos, E., Wheeler, J. C., & Vinko, J. 2012, ApJ, 746, 121

Chatzopoulos, E., Wheeler, J. C., & Couch, S. M. 2013a, ApJ, 776, 129
Chatzopoulos, E., Wheeler, J. C., Vinko, J., Horvath, Z. L., & Nagy, A. 2013b, ApJ, 773, 76
Chen, K.-J., Moriya, T. J., Woosley, S., et al. 2017, ApJ, 839, 85
Chen, T.-W., Smartt, S. J., Bresolin, F., et al. 2013, ApJ, 763, L28
Chen, T.-W., Smartt, S. J., Jerkstrand, A., et al. 2015, MNRAS, 452, 1567
Chen, K.-J., Woosley, S. E., & Sukhbold, T. 2016, ApJ, 832, 73
Chen, T.-W., Inserra, C., Fraser, M., et al. 2018, ApJ, 867, L31
Chevalier, R. A. 1982, ApJ, 258, 790
Chevalier, R. A., & Fransson, C. 1994, ApJ, 420, 268
Chevalier, R. A., & Irwin, C. M. 2011, ApJ, 729, L6
Chomiuk, L., Chornock, R., Soderberg, A. M., et al. 2011, ApJ, 743, 114
Chugai, N. N. 2009, MNRAS, 400, 866
Chugai, N. N., & Danziger, I. J. 1994, MNRAS, 268, 173
Colgate, S. A., & McKee, C. 1969, ApJ, 157, 623
Colgate, S. A., Petschek, A. G., & Kriese, J. T. 1980, ApJ, 237, L81
Cooke, J., Sullivan, M., Gal-Yam, A., et al. 2012, Nature, 491, 228
Dai, Z. G., & Lu, T. 1998a, A&A, 333, L87
Dai, Z. G., & Lu, T. 1998b, Physical Review Letters, 81, 4301
Dai, Z. G. 2004, ApJ, 606, 1000
Dai, Z. G., & Liu, R.-Y. 2012, ApJ, 759, 58
Dai, Z. G., Wang, S. Q., Wang, J. S., Wang, L. J., & Yu, Y. W. 2016, ApJ, 817, 132
De Cia, A., Gal-Yam, A., Rubin, A., et al. 2018, ApJ, 860, 100
D'Elia, V., Pian, E., Melandri, A., et al. 2015, A&A, 577, A116
Dessart, L., & Hillier, D. J. 2005, A&A, 437, 667
Dessart, L., Hillier, D. J., Waldman, R., Livne, E., & Blondin, S. 2012, MNRAS, 426, L76
Deustua, S., Goldhaber, G., Groom, D., et al. 1995, IAU Circ., 6270
Dexter, J., & Kasen, D. 2013, ApJ, 772, 30
Dong, S., Shappee, B. J., Prieto, J. L., et al. 2016, Science, 351, 257
Filippenko, A. V. 1997, ARA&A, 35, 309
Gal-Yam, A. 2012, Science, 337, 927
Gal-Yam, A. 2018, arXiv:1812.01428
Gal-Yam, A., Moon, D.-S., Fox, D. B., et al. 2004, ApJ, 609, L59
Gal-Yam, A., Mazzali, P., Ofek, E. O., et al. 2009, Nature, 462, 624
Galama, T. J., Vreeswijk, P. M., van Paradijs, J., et al. 1998, Nature, 395, 670
Gao, H., Lei, W.-H., You, Z.-Q., & Xie, W. 2016, ApJ, 826, 141
Gezari, S., Halpern, J. P., Grupe, D., et al. 2009, ApJ, 690, 1313
Ginzburg, S., & Balberg, S. 2012, ApJ, 757, 178
Greiner, J., Mazzali, P. A., Kann, D. A., et al. 2015, Nature, 523, 189
Heger, A., & Woosley, S. E. 2002, ApJ, 567, 532
Heger, A., Fryer, C. L., Woosley, S. E., Langer, N., & Hartmann, D. H. 2003, ApJ, 591, 288
Hjorth, J., & Bloom, J. S. 2012, The Gamma-Ray Burst - Supernova Connection, ed. C. Kouveliotou, R. A. M. J. Wijers, & S. Woosley, (Cambridge: Cambridge University Press), 169
Hjorth, J., Sollerman, J., Møller, P., et al. 2003, Nature, 423, 847
Howell, D. A., Sullivan, M., Nugent, P. E., et al. 2006, Nature, 443, 308
Inserra, C., Smartt, S. J., Jerkstrand, A., et al. 2013, ApJ, 770, 128
Inserra, C., Nicholl, M., Chen, T.-W., et al. 2017, MNRAS, 468, 4642
Inserra, C., Smartt, S. J., Gall, E. E. E., et al. 2018, MNRAS, 475, 1046
Ioka, K., Hotokezaka, K., & Piran, T. 2016, ApJ, 833, 110
Ivezić, Ž., Kahn, S. M., Tyson, J. A., et al. 2008, arXiv:0805.2366
Janka, H.-T. 2012, Annual Review of Nuclear and Particle Science, 62, 407
Janka, H.-T., Langanke, K., Marek, A., Martínez-Pinedo, G., & Müller, B. 2007, Phys. Rep., 442, 38
Kangas, T., Blagorodnova, N., Mattila, S., et al. 2017, MNRAS, 469, 1246
Kann, D. A., Schady, P., Olivares, F. E., et al. 2016, arXiv:1606.06791
Kasen, D., & Bildsten, L. 2010, ApJ, 717, 245
Kasen, D., & Woosley, S. E. 2009, ApJ, 703, 2205
Kotera, K., Phinney, E. S., & Olinto, A. V. 2013, MNRAS, 432, 3228
Kozyreva, A., & Blinnikov, S. 2015, MNRAS, 454, 4357
Law, N. M., Kulkarni, S. R., Dekany, R. G., et al. 2009, PASP, 121, 1395
Leloudas, G., Chatzopoulos, E., Dilday, B., et al. 2012, A&A, 541, A129
Leloudas, G., Fraser, M., Stone, N. C., et al. 2016, Nature Astronomy, 1, 0002
Liu, L.-D., Wang, L.-J., Wang, S.-Q., & Dai, Z.-G. 2018, ApJ, 856, 59
Liu, L.-D., Wang, S.-Q., Wang, L.-J., et al. 2017a, ApJ, 842, 26
Liu, Y.-Q., Modjaz, M., & Bianco, F. B. 2017b, ApJ, 845, 85
LSST Science Collaboration, Abell, P. A., Allison, J., et al. 2009, arXiv:0912.0201
Lundqvist, P., Kozma, C., Sollerman, J., & Fransson, C. 2001, A&A, 374, 629
Lunnan, R., Chornock, R., Berger, E., et al. 2013, ApJ, 771, 97
Lunnan, R., Chornock, R., Berger, E., et al. 2014, ApJ, 787, 138
Lunnan, R., Chornock, R., Berger, E., et al. 2015, ApJ, 804, 90
Lunnan, R., Chornock, R., Berger, E., et al. 2018, ApJ, 852, 81
MacFadyen, A. I., & Woosley, S. E. 1999, ApJ, 524, 262
Maeda, K., Tanaka, M., Nomoto, K., et al. 2007, ApJ, 666, 1069
Matsumoto, T., Nakauchi, D., Ioka, K., & Nakamura, T. 2016, ApJ, 823, 83
Mazzali, P. A., Deng, J., Nomoto, K., et al. 2006, Nature, 442, 1018
McCrum, M., Smartt, S. J., Rest, A., et al. 2015, MNRAS, 448, 1206
Melandri, A., Pian, E., Ferrero, P., et al. 2012, A&A, 547, A82
Metzger, B. D., Giannios, D., Thompson, T. A., Bucciantini, N., & Quataert, E. 2011, MNRAS, 413, 2031
Metzger, B. D., Margalit, B., Kasen, D., & Quataert, E. 2015, MNRAS, 454, 3311

Metzger, B. D., Thompson, T. A., & Quataert, E. 2007, ApJ, 659, 561
Miller, A. A., Chornock, R., Perley, D. A., et al. 2009, ApJ, 690, 1303
Miller, A. A., Silverman, J. M., Butler, N. R., et al. 2010, MNRAS, 404, 305
Minkowski, R. 1941, PASP, 53, 224
Moriya, T. J., Blinnikov, S. I., Tominaga, N., et al. 2013, MNRAS, 428, 1020
Moriya, T. J., Chen, T.-W., & Langer, N. 2017, ApJ, 835, 177
Moriya, T. J., Nicholl, M., & Guillochon, J. 2018, ApJ, 867, 113
Neill, J. D., Sullivan, M., Gal-Yam, A., et al. 2011, ApJ, 727, 15
Nicholl, M., & Smartt, S. J. 2016, MNRAS, 457, L79
Nicholl, M., Smartt, S. J., Jerkstrand, A., et al. 2013, Nature, 502, 346
Nicholl, M., Smartt, S. J., Jerkstrand, A., et al. 2014, MNRAS, 444, 2096
Nicholl, M., Smartt, S. J., Jerkstrand, A., et al. 2015, ApJ, 807, L18
Nicholl, M., Berger, E., Smartt, S. J., et al. 2016a, ApJ, 826, 39
Nicholl, M., Berger, E., Margutti, R., et al. 2016b, ApJ, 828, L18
Nicholl, M., Berger, E., Margutti, R., et al. 2017a, ApJ, 845, L8
Nicholl, M., Berger, E., Margutti, R., et al. 2017b, ApJ, 835, L8
Nicholl, M., Blanchard, P. K., Berger, E., et al. 2018, ApJ, 866, L24
Nicholl, M., Guillochon, J., & Berger, E. 2017c, ApJ, 850, 55
Ostriker, J. P., & Gunn, J. E. 1971, ApJ, 164, L95
Pastorello, A., Mattila, S., Zampieri, L., et al. 2008, MNRAS, 389, 113
Pastorello, A., Smartt, S. J., Botticella, M. T., et al. 2010, ApJ, 724, L16
Piro, A. L. 2015, ApJ, 808, L51
Piro, A. L., & Nakar, E. 2013, ApJ, 769, 67
Popov, D. V. 1993, ApJ, 414, 712
Quimby, R. M. 2014, in IAU Symposium, 296, Supernova Environmental Impacts, eds. A. Ray & R. A. McCray, 68
Quimby, R. M., Kulkarni, S. R., Kasliwal, M. M., et al. 2011, Nature, 474, 487
Quimby, R. M., Yuan, F., Akerlof, C., & Wheeler, J. C. 2013, MNRAS, 431, 912
Rakavy, G., & Shaviv, G. 1967, ApJ, 148, 803
Roy, R., Sollerman, J., Silverman, J. M., et al. 2016, A&A, 596, A67
Sanders, N. E., Soderberg, A. M., Valenti, S., et al. 2012, ApJ, 756, 184
Schlegel, E. M. 1990, MNRAS, 244, 269
Schlegel, E. M. 1996, AJ, 111, 1660
Schmidt, B., Tonry, J., Barris, B., et al. 2000, IAU Circ., 7516
Smartt, S. J. 2009, ARA&A, 47, 63
Smith, N., & McCray, R. 2007, ApJ, 671, L17
Smith, N., Li, W., Foley, R. J., et al. 2007, ApJ, 666, 1116
Smith, M., Sullivan, M., D'Andrea, C. B., et al. 2016, ApJ, 818, L8
Smith, N. 2017, Interacting Supernovae: Types IIn and Ibn, eds. A. W. Alsabti & P. Murdin, Handbook of Supernovae (Springer International Publishing AG), 403
Soker, N., & Gilkis, A. 2017, ApJ, 851, 95
Sollerman, J., Holland, S. T., Challis, P., et al. 2002, A&A, 386, 944
Stanek, K. Z., Matheson, T., Garnavich, P. M., et al. 2003, ApJ, 591, L17
Starling, R. L. C., Wiersema, K., Levan, A. J., et al. 2011, MNRAS, 411, 2792
Sukhbold, T., Ertl, T., Woosley, S. E., Brown, J. M., & Janka, H.-T. 2016, ApJ, 821, 38
Taddia, F., Sollerman, J., Leloudas, G., et al. 2015, A&A, 574, A60
Tolstov, A., Nomoto, K., Blinnikov, S., et al. 2017, ApJ, 835, 266
Toy, V. L., Cenko, S. B., Silverman, J. M., et al. 2016, ApJ, 818, 79
Ugliano, M., Janka, H.-T., Marek, A., & Arcones, A. 2012, ApJ, 757, 69
Umeda, H., & Nomoto, K. 2008, ApJ, 673, 1014
Usov, V. V. 1992, Nature, 357, 472
Valenti, S., Benetti, S., Cappellaro, E., et al. 2008, MNRAS, 383, 1485
Vinkó, J., Yuan, F., Quimby, R. M., et al. 2015, ApJ, 798, 12
Vreeswijk, P. M., Leloudas, G., Gal-Yam, A., et al. 2017, ApJ, 835, 58
Wang, S. Q., Wang, L. J., Dai, Z. G., & Wu, X. F. 2015a, ApJ, 807, 147
Wang, S. Q., Wang, L. J., Dai, Z. G., & Wu, X. F. 2015b, ApJ, 799, 107
Wang, L.-J., Han, Y.-H., Xu, D., et al. 2016a, ApJ, 831, 41
Wang, L.-J., Wang, S. Q., Dai, Z. G., et al. 2016b, ApJ, 821, 22
Wang, S. Q., Liu, L. D., Dai, Z. G., Wang, L. J., & Wu, X. F. 2016c, ApJ, 828, 87
Wang, L. J., Cano, Z., Wang, S. Q., et al. 2017a, ApJ, 851, 54
Wang, L. J., Wang, X. F., Cano, Z., et al. 2017b, arXiv:1712.07359
Wang, L. J., Yu, H., Liu, L. D., et al. 2017c, ApJ, 837, 128
Wang, S.-Q., Cano, Z., Wang, L.-J., et al. 2017d, ApJ, 850, 148
Wang, L. J., Wang, X. F., Wang, S. Q., et al. 2018, ApJ, 865, 95
Waxman, E., & Katz, B. 2017, Shock Breakout Theory, ed. A. W. Alsabti & P. Murdin, Handbook of Supernovae, eds. A. W. Alsabti & P. Murdin (Springer International Publishing AG), 967
Woosley, S. E. 1993, ApJ, 405, 273
Woosley, S. E. 2010, ApJ, 719, L204
Woosley, S. E., Blinnikov, S., & Heger, A. 2007, Nature, 450, 390
Woosley, S. E., & Bloom, J. S. 2006, ARA&A, 44, 507
Xu, D., de Ugarte Postigo, A., Leloudas, G., et al. 2013, ApJ, 776, 98
Yan, L., Quimby, R., Ofek, E., et al. 2015, ApJ, 814, 108
Yan, L., Quimby, R., Gal-Yam, A., et al. 2017, ApJ, 840, 57
Young, D. R., Smartt, S. J., Valenti, S., et al. 2010, A&A, 512, A70
Yu, Y. W., Zhu, J. P., Li, S. Z., L, H. J., & Zou, Y. C. 2017, ApJ, 840, 12
Zhang, B., & Mészáros, P. 2001, ApJ, 552, L35
Zhang, T., Wang, X., Wu, C., et al. 2012, AJ, 144, 131